Review and Analysis of Coaxial Magnetic Gear Pole Pair Count Selection Effects

Bryton Praslicka, *Student Member, IEEE*, Matthew C. Gardner, *Member*, *IEEE*, Matthew Johnson, *Member*, *IEEE*, and Hamid A. Toliyat, *Fellow, IEEE*

***Abstract*—Magnetic gears perform the same function as mechanical gears using magnetic fields instead of interlocking teeth. A review of the design processes used in the literature demonstrates that a critical design parameter, pole pair count, is often given inadequate consideration. In addition to reviewing existing prototypes, this paper uses a parametric simulation study to analyze the impacts of pole pair counts on gear performance and illustrate how the optimal pole counts vary with gear ratio and various design parameters. This paper also introduces new ripple factors, which better correlate with torque ripple than the cogging factor used in previous papers, and illustrates why designs with non-integer gear ratios tend to have much smaller torque ripples than designs with integer gear ratios. While selecting the pole counts to minimize symmetry can reduce torque ripple, designs without any symmetry are shown to experience unbalanced magnetic forces on each rotor. Thus, it is recommended to select pole counts that result in an even number of modulators but not an integer gear ratio. This paper also reveals that, for a fixed gear ratio, a nontrivial optimum pole count minimizes the electromagnetic losses.**

***Index Terms*—cogging factor, efficiency, finite element analysis, magnetic forces, magnetic gear, permanent magnet, pole pairs, radial flux, ripple factor, torque density, torque ripple**

I. Introduction

MAGNETIC gears transfer power between high-torque, low-speed rotation and low-torque, high-speed rotation using the modulated interaction of magnetic fields, instead of physical contact between interlocking teeth like mechanical gears. The potential advantages of magnetic gears include inherent overload protection, reduced maintenance, improved reliability, and physical isolation between the shafts. Thus, magnetically geared systems attempt to combine the reliability benefits of gearless, direct-drive machines with the system size and cost reduction benefits of mechanically geared systems. These potential advantages have resulted in significant recent interest in using magnetic gears in a range of applications. NASA built magnetic gear prototypes and concluded that magnetic gears may be able to achieve specific torques comparable to those of low-torque-level aircraft mechanical transmissions [1]-[4]. Prototype magnetic gears have also been developed for a variety of other potential uses, such as wind [5]-[7] and wave [8], [9] energy conversion, traction [10]-[13], space applications [14], and hybrid electric vehicle power split devices [15]. Additionally, some review studies suggest that magnetic gearing technology has potential in wind [16], [17], marine [18], and aerospace actuation applications [19]-[20].

Generally, radial flux coaxial (concentric) magnetic gears have achieved the highest experimentally demonstrated torque densities [2], [3], [21]. The radial flux coaxial topology is shown in Fig. 1(a), and its axial analog, which has not yet experimentally demonstrated the same torque densities [22]-[24], is shown in Fig. 1(b). A transverse flux coaxial magnetic gear has also been proposed [25], [26], but it has received relatively little interest, due to its low torque density [27].

This paper includes an extensive catalog of 63 coaxial magnetic gear and magnetically geared machine prototypes produced in the last 20 years [1], [2], [5]-[8], [10]-[15], [19], [22]-[24], [28]-[69]. Tables I and II describe the magnetic gear

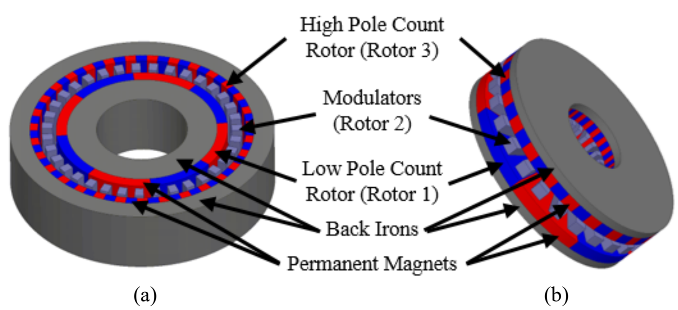

Fig. 1. Coaxial (a) radial flux and (b) axial flux magnetic gears with surface-mounted permanent magnets.

Manuscript received September 22, 2020. This work was supported in part by the U.S. Army Research Laboratory and was accomplished under Cooperative Agreement Number W911NF-18-2-0289. The views and conclusions contained in this document are those of the authors and should not be interpreted as representing the official policies, either expressed or implied, of the Army Research Laboratory or the U.S. Government. The U.S. Government is authorized to reproduce and distribute reprints for Government purposes notwithstanding any copyright notation herein."

B. Praslicka is with the Advanced Electric Machines and Power Electronics Lab at Texas A&M University, College Station, TX 77843 USA (e-mail: bryton.praslicka@tamu.edu).

M. C. Gardner was with the Advanced Electric Machines and Power Electronics Lab at Texas A&M University, College Station, TX 77843 USA. He is now with the University of Texas at Dallas, Dallas, TX 75080 USA (e-mail: Matthew.Gardner@utdallas.edu).

M. Johnson is with the U.S. Army Combat Capabilities Development Command Army Research Laboratory, College Station, TX 77843 USA (e-mail: matthew.c.johnson186.civ@mail.mil).

H. A. Toliyat is with the Advanced Electric Machines and Power Electronics Lab at Texas A&M University, College Station, TX 77843 USA (e-mail: toliyat@tamu.edu).

TABLE I
SUMMARY OF COAXIAL MAGNETIC GEAR PROTOTYPES

Source	Year Published	Gear Ratio	Volumetric Torque Density (kN*m/m^3)	Evaluated Multiple Pole Pair Counts	Prototype Pole Pair Counts [P_1, P_3, Q_2]	High Speed Rotor Torque Ripple <20%
[28]	2020	10.67	120	✓	3, 32, 35	No Report
[6]	2019	6.45	141	×	11, 60, 71	×
[7]	2019	9.14	135	×	7, 57, 64[a]	No Report
[29]	2019	4.67	74.29	✓	3, 11, 14[a]	✓
[30], [31]	2019, 2020	4	36.96	×	2, 8, 10[a]	No Report
[30], [31]	2019, 2020	4	35.08	×	2, 8, 10[a]	No Report
[30], [31]	2019, 2020	4	31.08	×	2, 8, 10[a]	No Report
[32]	2019	4.25	70.90	×	4, 17, 21	✓
[32]	2019	4.25	63.95	×	4, 17, 21	✓
[32]	2019	4.25	55.60	×	4, 17, 21	✓
[1]	2018	4.25	102.42	✓	4, 13, 17	No Report
[2], [3]	2018	4.83	162.52	✓	6, 23, 29	No Report
[33]	2018	15	142	×	2, 30, 32[a]	×
[34]	2018	6	37.77	×	1, 5, 6[a]	×
[35]	2018	7	32.10	✓	2, 12, 14[a]	✓
[36], [37]	2018	3.75	116.45	✓	4, 11, 15	No Report
[37]	2018	11	119.92	✓	2, 20, 22[a]	No Report
[14][b]	2017	44	47.4	×	–	No Report
[14][b]	2017	10	92.3	×	–	No Report
[14][b]	2017	75	37.1	×	–	No Report
[38]	2016	21	42.25	✓	1, 21, 22[a]	×
[38]	2016	21	41.1	✓	1, 21, 22[a, c]	✓
[39]	2016	3.83	53.49	×	6, 17, 23	No Report
[40]	2015	10.5	111.2	×	2, 21, 23	No Report
[41]	2015	4.17	3	×	6, 19, 25	No Report
[42]	2015	20	25	×	2, 40, 42[a]	No Report
[24]	2014	8	22.4	×	1, 8, 9	×
[43]	2014	4.25	130.4	×	4, 17, 21	✓
[9], [44]	2014	4.25	33	×	4, 13, 17	✓
[44]	2014	4.25	66.3	×	4, 13, 17	✓
[44]	2014	4.25	151.2	×	4, 13, 17	✓
[45]	2014	4.25	238.7	×	8, 26, 34[a]	✓
[46]	2013	5.5	36.94	×	4, 22, 26[a]	No Report
[14], [47][b]	2013, 2017	21	141.9	×	–	No Report
[48]	2013	10.5	62.16	×	2, 21, 23	✓
[49]	2013	10.5	57.82	✓	2, 21, 23	No Report
[50], [51]	2010, 2012	2.5	30.8	×	4, 10, 14[a]	✓
[52]	2012	10.33	12.3	×	3, 31, 34[a]	No Report
[53]	2011	12[d]	65.3	✓	4, 22, 26[a]	No Report
[54]	2011	5.5	42	×	4, 22, 26[a]	✓
[55]	2010	10.5	80.84	✓	2, 21, 23	No Report
[51]	2010	2.5	30.8	×	4, 10, 14[a, c]	✓
[56]	2009	4.25	95.36	×	4, 17, 21	✓
[56]	2009	4.25	108.29	×	4, 17, 21	✓
[57]	2009	7.33	53.34	×	3, 22, 25	No Report
[58]	2005	5.5	54.5	×	4, 22, 26[a]	No Report
[59]	2004	5.75	72	✓	4, 23, 27	No Report

[a]This prototype has symmetry.
[b]The pole pair counts of this prototype are not specified.
[c]This prototype has skew.
[d]Contra-rotating system.

and magnetically geared machine prototypes, respectively, and provide the associated references. For both of these tables, some cells are empty because the references did not provide the necessary information to determine these values. While several published reviews of magnetic gears address various topics, including wind energy [17], marine energy [18], torque density [20], [21], torsional stiffness [20], and opportunities and challenges for magnetic gears [70] and magnetically geared machines [71], Tables I and II show that a critical design aspect, pole count selection, is often given inadequate consideration, even in recently published works. Thus, some prototypes

TABLE II
SUMMARY OF COAXIAL MAGNETICALLY GEARED MACHINE PROTOTYPES

Source	Year Published	Gear Ratio	Volumetric Torque Density (kN*m/m^3)	Evaluated Multiple Pole Pair Counts	Prototype Pole Pair Counts [P_1, P_3, Q_2]	Output Rotor Torque Ripple <5%
[22]	2020	4.17	94.4	×	6, 19, 25	✓
[5]	2020	11.6	85.6	✓	5, 53, 58[a]	✓
[15]	2019	2.29[b]	44.6	✓	7, 9, 16[a]	✓
[19]	2019	7.75	46.2	✓	4, 27, 31	✓
[8]	2018	11.33	82.8	✓	6, 68, 74[a]	✓
[23]	2017	9.33	7.8	✓	3, 28, 31	✓
[34], [60]	2016	10.5	76.7	✓	2, 19, 21	✓
[61]	2016	7.33	138.7[c]	✓	3, 22, 25	✓
[62], [63]	2013, 2015	7.2	107	✓	5, 31, 36[a]	✓
[12], [13]	2012, 2015	9	99.7	✓	4, 32, 36[a]	No Report
[10], [11]	2009, 2013	8.83	92	✓	6, 53, 59	No Report
[64], [65]	2012, 2013	6.67	9.6	✓	3, 20, 23	×
[66]	2012	5.33[d]	81.9	×	3, 13, 16[a]	No Report
[67]	2009	7.33	87[c]	×	3, 22, 25	No Report
[68]	2008	11.5	60	×	2, 21, 23	✓
[69]	2008	7.33	–	×	3, 22, 25	No Report

[a]This prototype has symmetry
[b]Power split device (P_3 = 9, Q_2 = 16, and 7 stator pole pairs).
[c]Torque density based on 2D FEA; experimental results not provided
[d]Continuously variable transmission (P_1 = 3, P_3 = 13, and Q_2 = 16)

exhibited egregious torque ripple [24], [33], [34], [38], specifically because of poor pole pair count selection. While there are other means of reducing torque ripples, such as skewing [38], [51], [72], adjusting the pole pitches [73], adjusting the modulators' shape [74], [75], increasing the effective air gap between the Rotor 1 magnets and the modulators [35], or adjusting the rotor pole shapes [76], intelligently selecting the pole counts is a simple means to achieve a drastic reduction in torque ripple [8], [77], [78]. In addition to torque ripple, pole pair counts also have tremendous impacts on other performance aspects of the design, including slip torque [1], [2], [77], [79] and unbalanced magnetic forces on the rotors of a coaxial magnetic gear [8], [31], [33], [36]-[38], [80]. It has been observed that the optimal pole count changes depending on the magnet material [81], and the optimization objective [82]. Nonetheless, some papers neglect to adequately evaluate different pole count options, leading the authors to draw some misleading conclusions [83]-[86].

This paper is intended to serve as a reference for the effects of pole count selection on various aspects of coaxial magnetic gear performance. It explains and quantitatively illustrates the impact of pole count selection on slip torque, torque ripple, and unbalanced magnetic forces. It also presents a pole count selection strategy that avoids both unbalanced magnetic forces and egregious torque ripple. Additionally, this paper proposes a new ripple factor that correlates better with torque ripple than the cogging factor used in previous papers, especially when the Rotor 1 pole count is varied, and presents new conclusions on pole counts' impact on electromagnetic losses. Finally, this paper uses a parametric optimization study to illustrate the effects of different parameters on optimal pole counts. Throughout the analysis of these considerations, this paper also notes how inadequate investigation of pole counts has led to misleading conclusions in some previous papers.

II. Review of Pole Pair Selection Criteria

Each of the coaxial magnetic gear topologies shown in Fig. 1 consists of two permanent magnet (PM) rotors (Rotors 1 and 3) and a rotor with soft magnetic poles called modulators (Rotor 2). The number of modulators (Q_2) should be the sum of the pole pairs on Rotor 1 (P_1) and Rotor 3 (P_3), as in

$$Q_2 = P_1 + P_3. \tag{1}$$

Coaxial magnetic gears have different operating modes, which yield different gear ratios. However, the highest fixed gear ratio is achieved when the high pole count PM rotor (Rotor 3) is held stationary, yielding the gear ratio (G) given by

$$G|_{\omega_3=0} = \frac{\omega_1}{\omega_2} = \frac{Q_2}{P_1}, \tag{2}$$

where ω_1, ω_2, and ω_3 are the steady–state speeds of Rotors 1, 2, and 3, respectively. The other common operating mode involves holding the modulators (Rotor 2) fixed, which yields

$$G|_{\omega_2=0} = \frac{\omega_1}{\omega_3} = -\frac{P_3}{P_1}, \tag{3}$$

where the negative sign indicates that Rotors 1 and 3 rotate in opposite directions.

To analyze the impact of pole counts and corroborate the observations made throughout the remainder of this paper, numerous 2D finite element analysis (FEA) simulations of the coaxial radial flux magnetic gear with surface permanent magnet rotors illustrated in Fig. 1(a) were run using the baseline parameters in Table III and the results are plotted. Various pole and modulators counts were evaluated. All simulated designs in this paper use NdFeB N42 PMs and M47 laminated steel for the modulators and back irons.

A. *Pole Pair Count Selection for Minimal Torque Ripple*

Previous studies describe the impact of pole pair count on torque ripple in PM machines [87]. The cogging factor (C_T) is defined for PM machines as

$$C_T = \frac{2pQ}{\mathrm{LCM}(2p,Q)} = \mathrm{GCD}(2p,Q), \tag{4}$$

where $2p$ is the pole count, Q is the number of slots, LCM stands for least common multiple, and GCD stands for greatest common divisor. For a magnetic gear, the value of C_T will be the same if either P_1 or P_3 is used for p in (4) because of the relationship in (1). The magnitude of C_T provides a general indication of the amount of cogging torque in a PM machine [87] and has been adapted to indicate the amount of torque ripple in magnetic gears [9], [18], [36]-[38], [41], [49], [55], [59], [64], [68], [70], [72], [76], [83], [88]. The cogging factor is based on a principle of symmetry minimization in a PM machine. In permanent magnet machines, cogging torque is the torque present in the machine when the windings are deenergized. However, magnetic gears do not have windings that are energized or deenergized. Additionally, the torque ripple in a magnetic gear is generally independent of the average torque, as observed experimentally in [6], [7], [22]. Thus, "cogging torque" and "torque ripple" are often used interchangeably in the literature on magnetic gears. Fig. 2 illustrates the impact of gear ratio on C_T and on torque ripple as a percentage of the average torque on each rotor when P_1 is fixed at different values and the gear specified in Table III is operated with a fixed Rotor 3 at the maximum (slip) torque angle. Fig. 2 shows that integer gear ratios, especially even integer gear ratios, produce much larger torque ripples than non-integer gear ratios. If Rotor 2 is fixed and Rotor 3 is used as the low speed rotor, then the largest torque ripples will occur at odd integer gear ratios. Fig. 2(a) shows C_T for each of the cases characterized in Figs. 2(b) and 2(c). Comparing these plots reveals that applying the cogging factor to magnetic gears provides some correlation with the torque ripple when the value of P_1 is fixed (there are similar trends within lines of the same

TABLE III
MAGNETIC GEAR BASELINE GEOMETRIC PARAMETERS

Parameter	Value	Units
Outer radius (R_{Out})	100	mm
Rotor 1 back iron thickness (T_{BI1})	25	mm
Rotor 1 PM thickness (T_{PM1})	12	mm
Air gap thicknesses (T_{AG})	1	mm
Modulator thickness (T_{Mods})	10	mm
Rotor 3 PM thickness (T_{PM3})	9	mm
Rotor 3 back iron thickness (T_{BI3})	25	mm

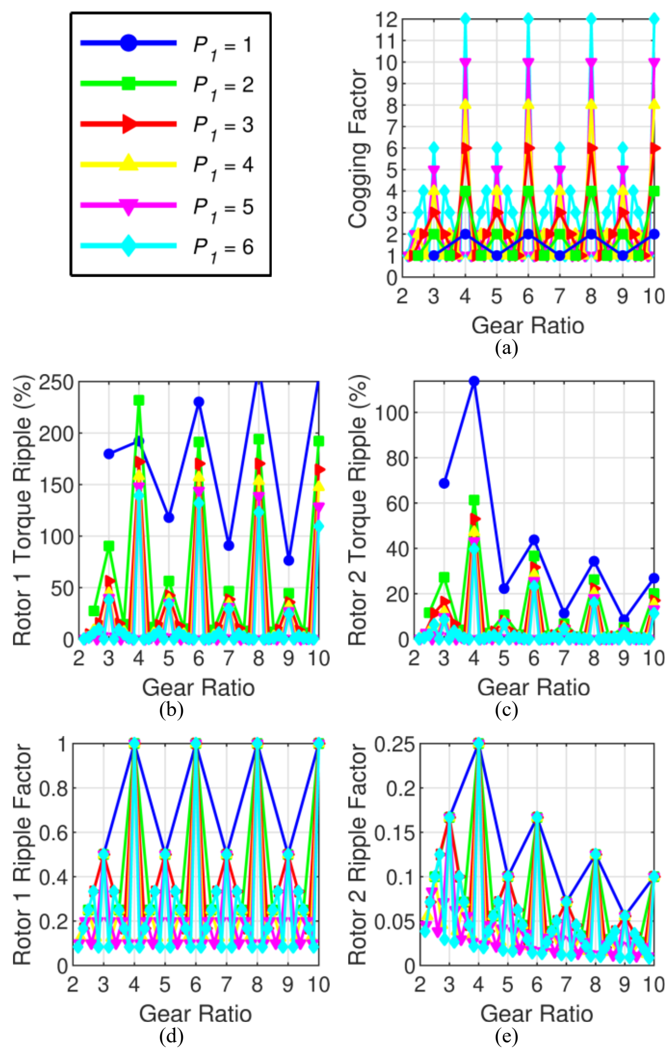

Fig. 2. (a) Cogging factor, (b) Rotor 1 torque ripple, (c) Rotor 2 torque ripple, (d) Rotor 1 ripple factor, and (e) Rotor 2 ripple factor for variations of the base design in Table III with different Rotor 1 pole pair counts and gear ratios.

color in Figs. 2(a), 2(b), and 2(c)). However, C_T does not accurately indicate how changes in P_1 affect the torque ripple (the relationships between lines of different colors are significantly different in Fig. 2(a) and in Figs. 2(b) and 2(c)).

Fig. 3 illustrates the torque on each Rotor 1 PM and the net torque on Rotor 1 for designs with different Rotor 3 pole pair counts as the gears operate at the slip torque angle for one full magnetic cycle. For the cases plotted in Fig. 3, a 95% Rotor PM fill factor is used instead of the 100% fill factor used for simulations in the rest of the paper. Whereas this slight reduction in fill factor does not have a huge impact on the net torque on Rotor 1, it does increase the difference between the PM torque waveforms, especially for Figs. 3(a) and 3(f), because it removes shared tangential boundaries. In the case of an odd integer gear ratio design according to (2), as in Figs. 3(a) and 3(f), there are only two groups of PM torque waveforms, and in the case of an even integer gear ratio according to (2), as in Figs. 3(b) and 3(e), the torque waveforms on all of the individual Rotor 1 PMs are in phase with each other, so the net torque displays a large ripple. For the design with a cogging factor of 1 (Fig. 3(c)), the torques on all of the individual PMs are out of phase with each other, so most of the variation cancels out, resulting in a very small net torque ripple. If a design has a cogging factor of 2 (Fig. 3(d)); this means that the gear has some symmetry and the torques of pairs of the individual PMs are in phase with each other, which produces an intermediate amount of net torque ripple. However, the designs in Figs. 3(e) and 3(f) also have cogging factors of 2 and 1 but demonstrate much larger torque ripples than Figs. 3(d) and 3(c), respectively. Thus, a better indicator of the torque ripple may be the extent to which the torque waveforms of the individual Rotor 1 PMs are out of phase with each other. Therefore, a new Rotor 1 ripple factor ($R_{F,1}$) can be defined as the design's symmetry factor divided by the number of Rotor 1 poles,

$$R_{F,1} = \frac{\mathrm{GCD}(2P_1,Q_2)}{2P_1} = \frac{C_T}{2P_1} = \frac{Q_2}{\mathrm{LCM}(2P_1,Q_2)}, \qquad (5)$$

where GCD stands for greatest common divisor. Similarly, a new Rotor 2 ripple factor ($R_{F,2}$) can be defined as

$$R_{F,2} = \frac{\mathrm{GCD}(2P_1,Q_2)}{Q_2} = \frac{C_T}{Q_2} = \frac{2P_1}{\mathrm{LCM}(2P_1,Q_2)}. \qquad (6)$$

As with the cogging factor, the Rotor 2 ripple factor has the same value, regardless of whether P_1 or P_3 is used. $R_{F,3}$ can be calculated similarly to $R_{F,1}$ by replacing P_1 with P_3. The ripple factor is the inverse of the number of poles (or modulators for Rotor 2) in the smallest symmetrical fraction of the model, so the ripple factor is inversely proportional to the number of distinct phase shifted torque waveforms illustrated in Fig. 3.

Figs. 2(d) and 2(e) depict these ripple factors, which show a better correlation with the torque ripples in Fig. 2(b) and (c) than the cogging factor defined by (4), especially when P_1 is varied. Integer gear ratios produce large torque ripples, as shown in some recent papers [24], [33], [34], [38], [73], [78], [84], [88]. While integer gear ratios may be required in certain scenarios, such as achieving a high gear ratio with a small radius [38], when possible, using a non-integer gear ratio is a simple way to reduce torque ripple. The ripple factor applies for any pole pair count, including $P_1 = 1$. In contrast, using the cogging factor alone can be misleading, as it suggests that a design with $P_1 = 1$ ($C_T = 1$ or $C_T = 2$) will yield low ripple [38], when in reality $P_1 = 1$ always yields an integer gear ratio and larger torque ripples than non-integer gear ratios [24], [38]. Comparing Fig. 3(e) and 3(f), which have $R_{F,1} = 1$ and $R_{F,1} = 0.5$, respectively, with Figs. 3(d) and 3(c), which have $R_{F,1} = 0.33$ and $R_{F,1} = 0.17$, respectively, demonstrates the improvement of $R_{F,1}$ over C_T in predicting the Rotor 1 torque ripple, especially when P_1 is varied.

Table IV provides experimental evidence from the literature for prototypes with measured torque ripple. Table IV does not include prototypes with skew or topologies which purposefully increase the effective air gap between the modulators and the Rotor 1 magnets as the purpose of Table IV is to relate pole counts with torque ripple only. The low speed rotor (LSR) ripple factor is calculated using RF_2 or RF_3, depending on which rotor is used as the low speed rotor. It should be noted that assembly problems, manufacturing tolerances, and measurement noise can introduce torque ripple into the

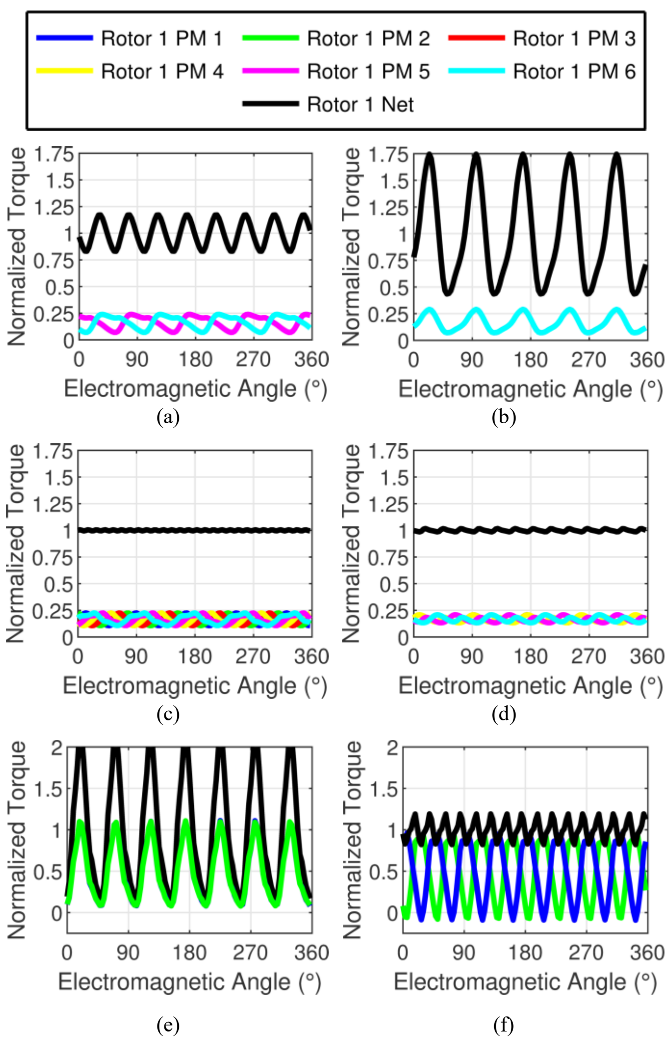

Fig. 3. The normalized torque on each Rotor 1 PM and the net torque on Rotor 1 for the base design with a Rotor 1 magnet fill factor of 0.95 with (a) $P_1 = 3$, $Q_2 = 15$, and $P_3 = 12$, (b) $P_1 = 3$, $Q_2 = 18$, and $P_3 = 15$, (c) $P_1 = 3$, $Q_2 = 17$, and $P_3 = 14$, and (d) $P_1 = 3$, $Q_2 = 16$, and $P_3 = 13$, (e) $P_1 = 1$, $Q_2 = 8$, and $P_3 = 7$, and (f) $P_1 = 1$, $Q_2 = 9$, and $P_3 = 8$.

TABLE IV
SUMMARY OF COAXIAL MAGNETIC GEAR PROTOTYPE TORQUE RIPPLE

Source	Pole Pair Counts [P_1, P_3, Q_2]	Low Speed Rotor	Gear Ratio	C_T	HSR Ripple Factor	LSR Ripple Factor	HSR Ripple	LSR Ripple
[28]	3, 32, 35	3	10.67	1	0.167	0.0156	–	3.9%
[22]	6, 19, 25	2	4.17	1	0.0833	0.0400	12.7%	3.2%
[6]	11, 60, 71	2	6.45	1	0.0455	0.0141	23%	2.4%
[33]	2, 30, 32	3	15	4	1	0.0667	84%	–
[34]	1, 5, 6	2	6	2	1	0.333	50%	110%
[38]	1, 21, 22	3	21	2	1	0.0476	146%	–
[44]	4, 13, 17	2	4.25	1	0.125	0.0588	10%	0.4%
[44]	4, 13, 17	2	4.25	1	0.125	0.0588	1%	0.2%
[45]	8, 26, 34	2	4.25	2	0.125	0.0588	1%	0.2%
[50]	4, 10, 14	3	2.5	2	0.250	0.100	2.5%	2.7%
[54]	4, 22, 26	3	5.5	2	0.250	0.0455	3%	11%
[8]	6, 68, 74	3	11.33	2	0.167	0.0147	–	1%
[34], [60]	2, 19, 21	2	10.5	1	0.250	0.0476	–	17%

measurements, which may dominate the results for cases with low ripple factors [6]. For example, in the previous large scale prototype tested by the authors in [8], shown in Fig. 4(a), the torque ripple on the LSR, shown in Fig. 4(b), appears to be dominated by measurement noise. Nevertheless, the results in Table IV, which are plotted in Fig. 5, reveal that the ripple factor is a better predictor of which designs will have low torque ripples on both the high speed rotor (HSR) and the LSR than the cogging factor.

B. *Unbalanced Magnetic Forces*

In [8], [31], [33], [37] and [38], the authors were alert to the need to select pole counts to create symmetry in the radial magnetic forces acting on each rotor. In [36], higher than expected mechanical losses were attributed to increased bearing friction resulting from unbalanced magnetic forces. In [37], unbalanced magnetic forces produced significant vibrations in a prototype. Fig. 6 shows the x-axis and y-axis components of the net magnetic force acting on Rotor 2 as the same gears characterized in Fig. 3 operate at the slip torque angle for one full magnetic cycle. The gear designs characterized in Figs. 3(a), 3(b), 3(d) and 3(e) exhibit symmetry; therefore, their corresponding traces in Fig. 6 indicate very small net unbalanced magnetic forces, which are not ideally present and simply an artifact of numerical modeling. The gear designs characterized in Figs. 3(c) and 3(f) do not have any symmetry and correspond to the cyan and green traces in Fig. 6. When there is no symmetry in a design, each of its rotors experiences an unbalanced net magnetic force that varies in magnitude and direction during the operation of the gear. This phenomenon was observed in the prototypes described in [6], [36], [37]. Thus, while the gear design corresponding to Fig. 3(d) has higher torque ripples than the design corresponding to Fig. 3(c), the pole pair counts associated with Fig. 3(d) may produce a more desirable design, due to the net cancellation of radial magnetic forces.

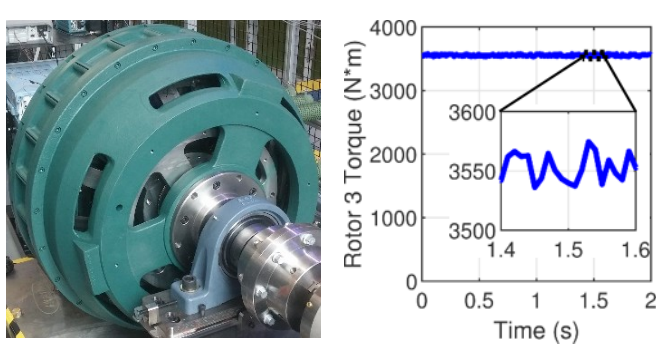

(a) (b)

Fig. 4. (a) Previous radial flux coaxial magnetically geared machine prototype [8] and (b) the experimental torque ripple data at a Rotor 3 speed of 30 rpm [8].

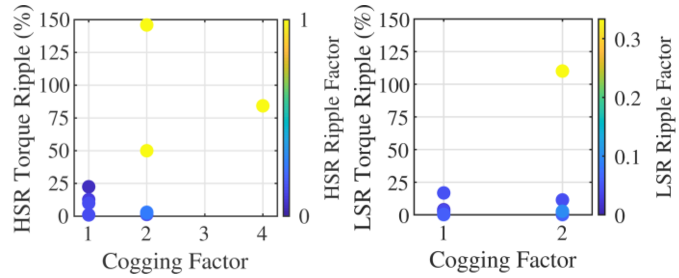

(a) (b)

Fig. 5. Experimentally measured (a) high speed rotor torque ripple and (b) low speed rotor torque ripple versus the cogging factors and ripple factors of the designs.

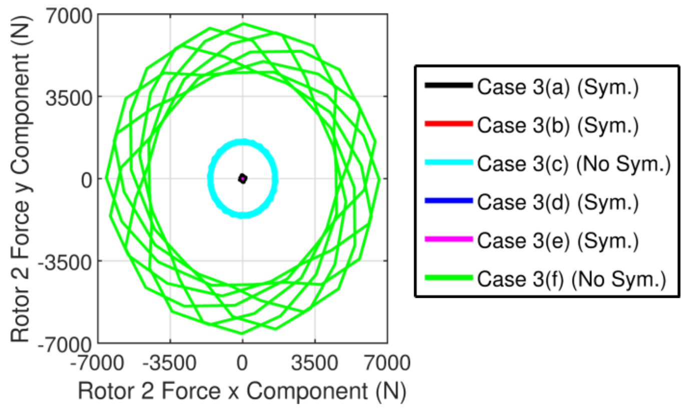

Fig. 6. X-axis and y-axis components of the net magnetic forces acting on Rotor 2 in the magnetic gear designs characterized in Fig. 3. Note that all the cases with symmetry (Sym.) form one dot at the origin.

For a radial (or transverse) flux coaxial magnetic gear, if $2P_1$, $2P_3$, and Q_2 have a common divisor greater than 1, such as 3 in the examples mentioned by [38] ($P_1 = 3$, $P_3 = 12$, and $Q_2 = 15$) and [80] ($P_1 = 6$, $P_3 = 9$, and $Q_2 = 15$), then symmetry exists, and the radial magnetic forces on each rotor will be balanced.

However, simply choosing P_1 and P_3 such that (1) yields an even value of Q_2 ensures that there will be symmetry in the design, eliminating unbalanced magnetic forces. When Rotor 3 is fixed (Rotor 2 serves as the low–speed rotor),

$$P_3|_{\omega_3=0} = \begin{cases} (G_{Int}-1)P_1+1 & \text{for } G_{Int}P_1 \text{ odd} \\ (G_{Int}-1)P_1+2 & \text{for } G_{Int}P_1 \text{ even}\end{cases}, \quad (7)$$

which was introduced in [89], can be implemented to select P_3 values for a given integer part of the gear ratio (G_{Int}) and a P_1 value. Then, (1) determines Q_2, and (2) determines the exact gear ratio (G), including the fractional part. If Rotor 3 is used as the low–speed rotor, then

$$P_3|_{\omega_2=0} = \begin{cases} G_{Int}P_1+1 & \text{for } (G_{Int}+1)P_1 \text{ odd} \\ G_{Int}P_1+2 & \text{for } (G_{Int}+1)P_1 \text{ even}\end{cases} \quad (8)$$

can be used to select pole pair combinations and (1) can still be used to determine modulator piece count, as was done in [81]. In this case, (3) determines the exact gear ratio. For $G_{Int} > 1$ and $P_1 > 2$, (7) and (8) always yield non-integer gear ratios and an even number of modulators, which eliminates designs with egregiously large torque ripple or unbalanced magnetic forces.

Similarly, axial flux coaxial magnetic gears without symmetry will experience off-axis torques. These off-axis torques may result in accelerated wear on the bearings, which already bear the significant axial loading resulting from the axial magnetic forces inherent in this topology. As with radial and transverse flux gears, these off-axis torques can ideally be eliminated by selecting pole counts that yield some degree of symmetry. Therefore, (7) or (8) also apply when designing an axial flux coaxial magnetic gear.

III. Optimal Pole Pair Counts

A parametric 2D FEA simulation study was used to characterize how pole pair counts impact a radial flux coaxial magnetic gear's slip torque and efficiency. All simulations assumed a fixed Rotor 3 (Rotor 2 serves as the low-speed rotor) and used the baseline parameters in Table III.

A. Torque Transmission Capability

Fig. 7 depicts the impact of the pole counts on the slip torque of the base design. This shows significantly different trends when P_1 is fixed and when P_1 is varied. If P_1 is allowed to vary, the torque is maximized near the minimum considered gear ratio, as in [90] and [91]. However, because some previous studies fixed P_1, they concluded that there is a larger optimal gear ratio [83]-[85]. Had these studies evaluated multiple values of P_1, they would have achieved higher torques at lower gear ratios, which result in more similar pole counts on both rotors and thus enable better simultaneous optimization of the pole counts on both rotors if pole count is considered as a design variable.

Fig. 7 illustrates that the Rotor 1 pole count for optimal torque transmission decreases as the gear ratio increases, which agrees with [79], [81], [90], and [91]. This mitigates the extent to which the Rotor 3 pole count exceeds its optimal value (an excessively high Rotor 3 pole count results in excessively high leakage flux). The optimal pole count is expected to vary with other parameters of a magnetic gear design, as well. Thus, a parametric 2D FEA study was conducted using the base design specified in Table III and varying individual design parameters one at a time along with P_1 to demonstrate how the optimal pole pair count varies depending on the geometry of the design. For these simulations, (7) was used to determine P_3 with $G_{Int} = 4$. Specific torque, which is defined as the Rotor 2 slip torque divided by the gear's total magnetically active mass, was used to compare designs. Figs. 8-12 show the results using normalized specific torque to generalize the observed design trends.

Fig. 8(a) reveals that the optimal pole count increases as the outer radius increases, which agrees with [77], [82], and [89]. This can be explained by considering that the arc length of the effective flux path increases as the radius increases. Thus, as the outer radius increases, a higher pole count is required to optimize the tradeoff between increasing the angular derivative of the magnetic coenergy and decreasing the amount of tangential leakage flux between adjacent poles in the gear. Fig. 8(b) shows that this tradeoff tends to keep the optimal pole arc on the outside of the Rotor 1 PMs roughly constant as the outer radius is increased.

Fig. 9 shows that as the Rotor 1 PM thickness increases, the optimal pole count decreases, which agrees with [82] and [89]. Similarly, as the Rotor 3 PM thickness increases, the optimal

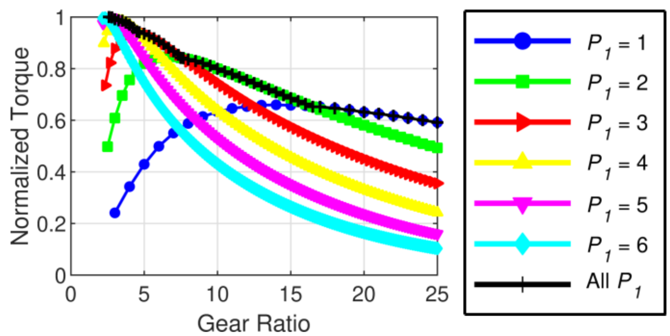

Fig. 7. Impact of gear ratio and Rotor 1 pole pair count on the normalized Rotor 2 slip torque of the base design defined in Table III.

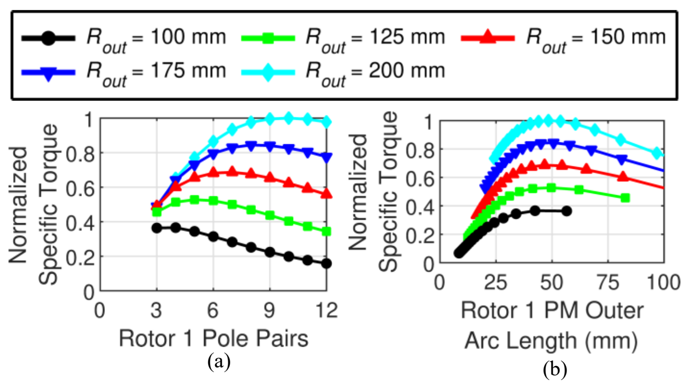

Fig. 8. Impact of Rotor 1 (a) pole pair count or (b) PM outer arc length on the normalized specific torque at various outer radii with $G_{Int} = 4$.

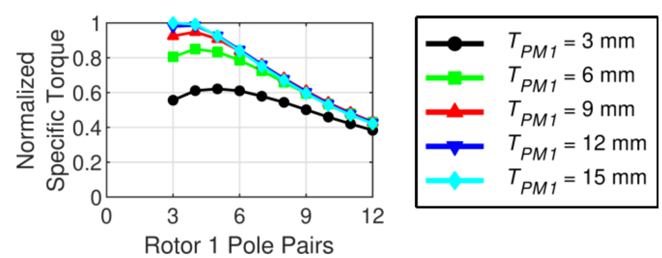

Fig. 9. Impact of Rotor 1 pole pair count on the normalized specific torque at various Rotor 1 magnet thicknesses with $G_{Int} = 4$.

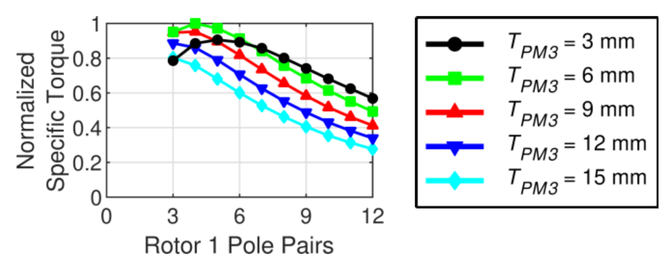

Fig. 10. Impact of Rotor 1 pole pair count on the normalized specific torque at various Rotor 3 magnet thicknesses with $G_{Int} = 4$.

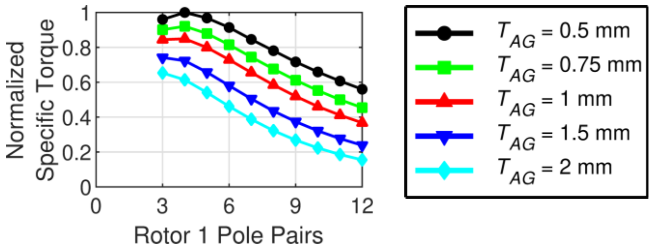

Fig. 11. Impact of Rotor 1 pole pair count on the normalized specific torque at various air gap thicknesses with $G_{Int} = 4$.

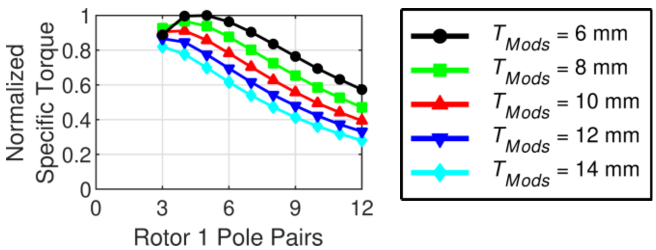

Fig. 12. Impact of Rotor 1 pole pair count on the normalized specific torque at various modulator thicknesses with $G_{Int} = 4$.

pole count decreases. In Fig. 10, as with the Rotor 1 PMs, thicker Rotor 3 PMs lead to lower optimal pole counts. Fig. 11 shows that the optimal pole count also decreases as the air gap increases. Figs. 9-11 indicate that as the effective air gap thickness (the physical air gaps plus the magnet thicknesses) increases, the optimal pole count decreases. This trend occurs because increasing the effective air gap increases the amount of leakage flux; thus, lower pole counts are required to increase the pole arcs and achieve the optimal balance between decreasing the amount of leakage flux and increasing the angular derivative of the magnetic coenergy.

Fig. 12 indicates that increasing the modulator thickness also decreases the optimal pole pair count, which is in concordance with [90]. This trend occurs because increasing the modulator thickness results in radially longer slots, which leads to more leakage flux. Consequently, the pole counts should be decreased in order to counteract this effect. Additionally, increasing the modulator thickness with a fixed outer radius pushes the inner air gap radius inward (making it smaller), which also lowers the optimal pole count.

It is well understood in the literature that end effects make a significant impact on magnetic gear performance [92]. In [82] it was found that 3D effects may have a small effect on the optimal parameters. Thus, 3D end effects may shift the trends found in Figs. 7-12; however, the general patterns regarding the relationships between geometric parameters and the optimal pole pair counts will not be fundamentally altered.

B. Losses

To evaluate the impact of pole pair counts on losses, the base designs were simulated using transient 2D FEA with Rotor 2 rotating at 100 rpm and Rotor 1 rotating according to the gear ratio. The results in Fig. 13 demonstrate that, for a fixed P_1 value, increasing the gear ratio increases the losses after Q_2 exceeds a small initial value. This occurs because increasing the gear ratio with a fixed P_1 value and a fixed ω_2 affects the amplitude of the flux density in the gear and increases the

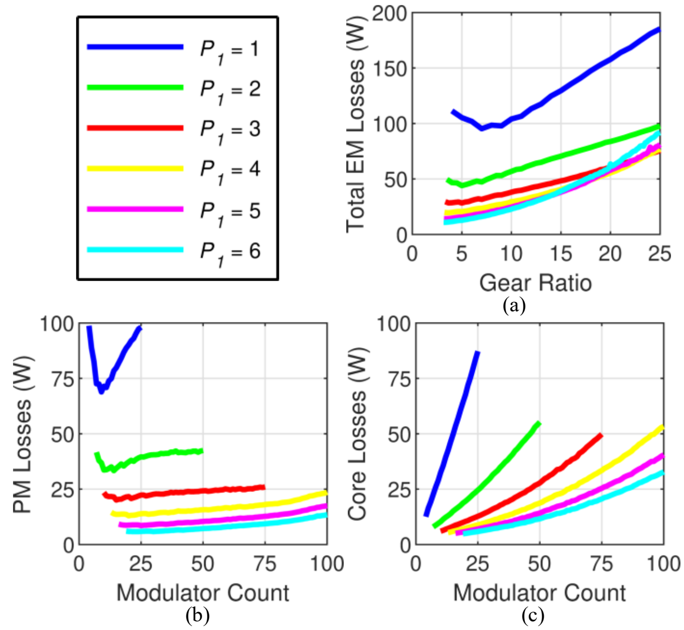

Fig. 13. (a) Variation of the base design's total electromagnetic (EM) losses with gear ratio and Rotor 1 pole pair count. Variation of the base design's (b) PM losses and (c) soft magnetic material core losses with modulator count and Rotor 1 pole pair count.

temporal frequencies of the magnetic flux density spatial harmonics (since a higher gear ratio results in a higher ω_1 for a fixed ω_2 and a higher ω_1 with a fixed P_1 value results in a higher electromagnetic Rotor 1 speed). Alternatively, if Q_2 and ω_2 are fixed, then the temporal frequencies of the gear's magnetic flux density spatial harmonics are fixed and increasing P_1 reduces the gear's electromagnetic losses. Increasing P_1 segments the Rotor 1 PMs, yielding smaller PM arc lengths, which reduces eddy currents and the lengths of the Rotor 1 flux paths. The shorter Rotor 1 flux paths result in less asynchronous flux in Rotor 3.

IV. Conclusion

Table I reveals that a critical coaxial magnetic gear design element, pole count selection, is often given inadequate consideration. Even for the design of some recent prototypes, only a single set of pole pair counts was evaluated, which yielded relatively large torque ripples [24], [33], [34].

Therefore, this paper provides a reference describing various criteria to consider when selecting pole counts for magnetic gears. The paper uses FEA results and a review of results in the literature to summarize, quantitatively illustrate, and explain the impacts of magnetic gear pole counts on slip torque, torque ripple, magnetic forces, and losses.

FEA analysis summarized in Fig. 2 and experimental torque ripple results in the literature (Table IV) demonstrate that designs with integer gear ratios, especially designs with Q_2 as an even multiple of P_1, have significantly larger torque ripple than designs with non-integer gear ratios. Fig. 3 illustrates an explanation for this phenomenon by plotting the torque waveforms for each pole on Rotor 1. Based on this explanation, (5) and (6) introduce new ripple factors based on the number of distinct torque waveforms for the poles or modulators. Figs. 2

and 5 and Table IV use FEA and experimental results to corroborate the hypothesis that the ripple factors better predict which designs will have low torque ripple than the traditional cogging factor.

The FEA results presented in Fig. 6 and the literature demonstrate that unbalanced magnetic forces in radial flux magnetic gears can be significant but can be easily eliminated by selecting pole counts that result in symmetry. In axial flux magnetic gears, symmetry eliminates the off-axis torques. As torque ripple is minimized by choosing pole counts that do not result in symmetry but symmetry is desirable for eliminating unbalanced magnetic forces or off-axis torques, (7) and (8) provide heuristics for selecting pole counts which yield a design compromise that keeps torque ripple relatively low, while eliminating unbalanced magnetic forces or off-axis torques. These equations yield pole counts which eliminate unbalanced magnetic forces or off-axis torques by imposing some symmetry yet also preclude pole count selections that yield integer gear ratios for designs with $P_1 > 1$.

The FEA results presented in Fig. 7 and the literature demonstrate that, if both P_1 and P_3 are allowed to vary, the maximum torque density is achieved with a relatively low gear ratio. This contradicts conclusions in some papers where P_1 was fixed [83]-[85]. Additionally, the optimal P_1 value decreases as the gear ratio increases. The FEA results presented in Fig. 8 and the literature show that the optimal P_1 value increases with outer radius. If other geometric parameters besides the outer radius are fixed, Fig. 8(b) demonstrates that the optimal P_1 value will change to maintain an approximately constant Rotor 1 PM outer arc length. The FEA results presented in Figs. 9-12 and the literature demonstrate that increasing the radial thickness of the PMs, air gaps, or modulators reduces the optimal pole counts.

FEA results presented in Fig. 13 illustrate that increasing the gear ratio with a fixed P_1 value increases a gear's electromagnetic losses (after some initial small modulator count is exceeded), but, if the gear ratio is fixed, then increasing the pole counts (up to some nontrivial value) can reduce the electromagnetic losses. Thus, especially at low gear ratios, increasing the Rotor 1 pole count (up to some optimal value) can increase the efficiency because this both increases the design's slip torque (up to some optimal value) and reduces its electromagnetic losses.

This paper's key contributions and results can be summarized as follows:

- Tables I and II provide an extensive audit of coaxial magnetic gear and magnetically geared machine prototypes, with a focus on pole pair count selections.
- Integer gear ratios produce significant torque ripple, and the reason for this phenomenon is illustrated in Fig. 3.
- Equations (5) and (6) introduce new ripple factors, and Figs. 2 and 5 and Table IV use FEA and experimental results to demonstrate that the ripple factors are better predictors of which magnetic gear designs will have low torque ripples than the traditionally used cogging factor.
- Equations (7) and (8) provide heuristics for selecting pole counts which yield a design compromise that keeps torque ripple relatively low, while eliminating unbalanced magnetic forces.

Acknowledgment

Portions of this research were conducted with the advanced computing resources provided by Texas A&M High Performance Research Computing. The authors would also like to thank ANSYS for their support of the EMPE lab through the provision of FEA software.

References

[1] V. Asnani, J. Scheidler, and T. Tallerico, "Magnetic gearing research at NASA," in *Proc. of AHS Intl. 74th Annual Forum*, 2018, pp. 1–14.

[2] J. Scheidler, V. Asnani and T. Tallerico, "NASA's magnetic gearing research for electrified aircraft propulsion," in *Proc. AIAA/IEEE Elect. Aircraft Technol. Symp.*, 2018, pp. 1-12.

[3] J. Scheidler, Z. Cameron and T. Tallerico, "Dynamic testing of a high-specific-torque concentric magnetic gear," NASA Glenn Res. Center, Cleveland, OH, USA, Tech. Rep. GRC–E–DAA–TN68758, May 2019.

[4] T. F. Tallerico, Z. A. Cameron, J. J. Scheidler and H. Hasseeb, "Outer stator magnetically-geared motors for electrified urban air mobility vehicles," in *Proc. AIAA/IEEE Elect. Aircraft Technol. Symp.*, 2020, pp. 1-25.

[5] A. B. Kjaer, S. Korsgaard, S. S. Nielsen, L. Demsa and P. O. Rasmussen, "Design, fabrication, test, and benchmark of a magnetically geared permanent magnet generator for wind power generation," *IEEE Trans. Energy Convers.*, vol. 35, no. 1, pp. 24-32, Mar. 2020.

[6] K. Li, S. Modaresahmadi, W. B. Williams, J. D. Wright, D. Som and J. Z. Bird, "Designing and experimentally testing a magnetic gearbox for a wind turbine demonstrator," *IEEE Trans. Ind. Appl.*, vol. 55, no. 4, pp. 3522-3533, Jul.-Aug. 2019.

[7] K. Li *et al.*, "Electromagnetic analysis and experimental testing of a flux focusing wind turbine magnetic gearbox," *IEEE Trans. Energy Convers.*, vol. 34, no. 3, pp. 1512-1521, Sep. 2019.

[8] M. Johnson, M. C. Gardner, H. A. Toliyat, S. Englebretson, W. Ouyang, and C. Tschida, "Design, construction, and analysis of a large scale inner stator radial flux magnetically geared generator for wave energy conversion," *IEEE Trans. Ind. Appl.*, vol. 54, no. 4, pp. 3305-3314, Jul./Aug. 2018.

[9] K. K. Uppalapati, J. Z. Bird, D. Jia, J. Garner and A. Zhou, "Performance of a magnetic gear using ferrite magnets for low speed ocean power generation," in *Proc. IEEE Energy Convers. Congr. and Expo.*, 2012, pp. 3348-3355.

[10] P. O. Rasmussen, H. H. Mortensen, T. N. Matzen, T. M. Jahns and H. A. Toliyat, "Motor integrated permanent magnet gear with a wide torque-speed range," in *Proc. IEEE Energy Convers. Congr. and Expo.*, 2009, pp. 1510-1518.

[11] P. O. Rasmussen, T. V. Frandsen, K. K. Jensen and K. Jessen, "Experimental evaluation of a motor-integrated permanent-magnet gear," *IEEE Trans. Ind. Appl.*, vol. 49, no. 2, pp. 850-859, Mar.-Apr. 2013.

[12] T. V. Frandsen, P. O. Rasmussen and K. K. Jensen, "Improved motor intergrated permanent magnet gear for traction applications," in *Proc. IEEE Energy Convers. Congr. and Expo.*, 2012, pp. 3332-3339.

[13] T. V. Frandsen *et al.*, "Motor Integrated Permanent Magnet Gear in a Battery Electrical Vehicle," *IEEE Trans. Ind. Appl.*, vol. 51, no. 2, pp. 1516-1525, March-April 2015.

[14] J. Esnoz-Larraya *et al.*, "OPTIMAGDRIVE: high-performance magnetic gears development for space applications," *European Space Mechanisms and Tribology Symp.*, 2017.

[15] P. Chmelicek, S. D. Calverley, R. S. Dragan, and K. Atallah, "Dual rotor magnetically geared power split device for hybrid electric vehicles," *IEEE Trans. Ind. Appl.*, vol. 55, no. 2, pp. 1484-1494, Mar./Apr. 2019.

[16] H. Polinder, J. A. Ferreira, B. B. Jensen, A. B. Abrahamsen, K. Atallah and R. A. McMahon, "Trends in wind turbine generator systems," *IEEE J. Emerg. Sel. Topics Power Electron.*, vol. 1, no. 3, pp. 174-185, Sept. 2013

[17] R-J. Wang and S. Gerber, "Magnetically geared wind generator technologies: Opportunities and challenges," *Appl. Energy*, vol. 136, pp. 817-826, 2014.

[18] B. McGilton, R. Crozier, A. McDonald and M. Mueller, "Review of magnetic gear technologies and their applications in marine energy," *IET Renew. Power Generation*, vol. 12, no. 2, pp. 174-181, 5 2 2018.

[19] R. S. Dragan, R. E. Clark, E. K. Hussain, K. Atallah and M. Odavic, "Magnetically geared pseudo direct drive for safety critical applications," *IEEE Trans. Ind. Appl.*, vol. 55, no. 2, pp. 1239-1249, Mar.-Apr. 2019.

[20] G. Puchhammer, "Magnetic Gearing Versus Conventional Gearing in Actuators for Aerospace Applications," Karl Rejlek GmbH, Vienna, Austria, Tech. Rep. NASA/CP–2014–217519, May 2014.

[21] K. Li and J. Z. Bird, "A review of the volumetric torque density of rotary magnetic gear designs," in *Proc. Int. Conf. Elec. Mach.*, 2018, pp. 2016-2022.

[22] M. B. Kouhshahi *et al.*, "An axial flux focusing magnetically geared generator for low input speed applications," *IEEE Trans. Ind. Appl.*, vol. 56, no. 1, pp. 138-147, Jan.-Feb. 2020.

[23] M. Johnson, M. C. Gardner and H. A. Toliyat, "Design and analysis of an axial flux magnetically geared generator," *IEEE Trans. Ind. Appl.*, vol. 53, no. 1, pp. 97-105, Jan.-Feb. 2017.

[24] M. Johnson, A. Shapoury, P. Boghrat, M. Post and H. A. Toliyat, "Analysis and development of an axial flux magnetic gear," in *Proc. IEEE Energy Convers. Congr. and Expo.*, 2014, pp. 5893-5900.

[25] Y. Li, J. Xing, K. Peng, and Y. Lu, "Principle and simulation analysis of a novel structure magnetic gear," in *Proc. Int. Conf. Elec. Mach. And Sys.*, pp. 3845-3849.

[26] D. Zhu, F. Yang, Y. Du, F. Xiao and Z. Ling, "An axial-field flux-modulated magnetic gear," *IEEE Trans. Appl. Supercond.*, vol. 26, no. 4, pp. 1-5, June 2016.

[27] W. Bomela, J. Z. Bird, and V. M. Acharya, "The performance of a transverse flux magnetic gear," *IEEE Trans. Magn.*, vol. 50, no. 1, pp. 1-4, 2014.

[28] S. S. Nielsen, R. K. Holm, N. I. Berg and P. O. Rasmussen, "Magnetically geared conveyor drive unit - an updated version," in *Proc. IEEE Energy Convers. Congr. and Expo.*, 2020, pp. 285-292.

[29] M. C. Gardner, M. Johnson and H. A. Toliyat, "Performance impacts of practical fabrication tradeoffs for a radial flux coaxial magnetic gear with Halbach arrays and air cores," in *Proc. IEEE Energy Convers. Congr. Expo.*, 2019, pp. 3129-3136.

[30] M. Kowol, J. Kołodziej, M. Jagieła and M. Łukaniszyn, "Impact of Modulator designs and materials on efficiency and losses in radial passive magnetic gear," *IEEE Trans. Energy Conv.*, vol. 34, no. 1, pp. 147-154, Mar. 2019.

[31] M. Kowol, J. Kołodziej, R. Gabor, M. Łukaniszyn and M. Jagieła, "On-Load characteristics of local and global forces in co-axial magnetic gear with reference to additively manufactured parts of modulator," *Energies*, vol. 13, no. 12, pp. 1-18, Jun. 2020.

[32] L. Jian, Z. Deng, Y. Shi, J. Wei and C. C. Chan, "The mechanism how coaxial magnetic gear transmits magnetic torques between its two rotors: detailed analysis of torque distribution on modulating ring," *IEEE/ASME Trans. Mechatronics*, vol. 24, no. 2, pp. 763-773, April 2019.

[33] S. S. Nielsen, R. K. Holm, P. O. Rassmussen, "Conveyor system with a highly integrated permanent magnet gear and motor," in *Proc. IEEE Energy Convers. Congr. Expo.*, Sep. 2018, pp. 2359-2366.

[34] S. Gerber and R. Wang, "Cogging torque definitions for magnetic gears and magnetically geared electrical machines," *IEEE Trans. Magn.*, vol. 54, no. 4, pp. 1-9, Apr. 2018.

[35] X. Li, M. Cheng and Y. Wang, "Analysis, design and experimental verification of a coaxial magnetic gear using stationary permanent-magnet ring," *IET Elec. Power Appl.*, vol. 12, no. 2, pp. 231-238, 2 2018.

[36] A. Matthee, R. Wang, C. J. Agenbach, D. N. J. Els and M. J. Kamper, "Evaluation of a magnetic gear for air-cooled condenser applications," in *IET Elec. Power Appl.*, vol. 12, no. 5, pp. 677-683, 5 2018.

[37] C. J. Agenbach, D. N. J. Els, R. J. Wang and S. Gerber, "Force and vibration analysis of magnetic gears," in *Proc. IEEE Int. Elect. Mach. Drives Conf.*, 2018, pp. 752-758.

[38] G. Jungmayr, J. Loeffler, B. Winter, F. Jeske and W. Amrhein, "Magnetic gear: radial force, cogging torque, skewing, and optimization," *IEEE Trans. Ind. Appl.*, vol. 52, no. 5, pp. 3822-3830, Sept.-Oct. 2016.

[39] N. Iwasaki, M. Kitamura and Y. Enomoto, "Optimal design of permanent magnet motor with magnetic gear and prototype verification," *Elect. Eng. Jpn.*, vol. 194, no. 1, pp 60-69, Jan. 2016.

[40] A. Matthee, S. Gerber, R-J. Wang, "A high performance concentric magnetic gear", in *Proc. Southern African Universities Power Eng. Conf.*, pp. 203-207, 2015

[41] M. Tsai and L. Ku, "3-D printing-based design of axial flux magnetic gear for high torque density," *IEEE Trans. Magn.*, vol. 51, no. 11, pp. 1-4, Nov. 2015.

[42] J. L. Perez-Diaz *et al.*, "Performance of magnetic-superconductor non-contact harmonic drive for cryogenic space applications," *Machines,* vol. 3, no. 3, pp. 138-156, July 2015.

[43] L. Jing, L. Liu, M. Xiong and D. Feng, "Parameters analysis and optimization design for a concentric magnetic gear based on sinusoidal magnetizations," *IEEE Trans. Appl. Supercond.*, vol. 24, no. 5, pp. 1-5, Oct. 2014.

[44] K. K. Uppalapati, W. B. Bomela, J. Z. Bird, M. D. Calvin and J. D. Wright, "Experimental evaluation of low-speed flux-focusing magnetic gearboxes," *IEEE Trans. Ind. Appl.*, vol. 50, no. 6, pp. 3637-3643, Nov.-Dec. 2014.

[45] K. K. Uppalapati, J. Z. Bird, J. Wright, J. Pitchard, M. Calvin and W. Williams, "A magnetic gearbox with an active region torque density of 239Nm/L," in *Proc. IEEE Energy Convers. Congr. and Expo.*, 2014, pp. 1422-1428.

[46] T. Fujita *et al.*, "Surface magnet gears with a new magnet arrangement and optimal shape of stationary pole pieces," *J. Electromagn. Anal. Appl.*, vol. 5, no. 6, pp. 243-249, 2013.

[47] J. L. Perez-Diaz *et al.*, "Magnetic non-contact harmonic drive," in *Proc. ASME Int. Mech. Eng. Convers. Congr. and Expo.*, 2013, pp. 1-4.

[48] S. Gerber and R. Wang, "Evaluation of a prototype magnetic gear," *Proc. Int. Conf. Ind. Technol.*, 2013, pp. 319-324.

[49] R. Zanis, A. Borisavljevic, J. W. Jansen and E. A. Lomonova, "Modeling, design and experimental validation of a small-sized magnetic gear," in *Proc. Int. Conf. Elec. Mach. And Sys.*, 2013, pp. 560-565.

[50] N. Niguchi and K. Hirata, "Cogging torque analysis of magnetic gear," *IEEE Trans. Ind. Electron.*, vol. 59, no. 5, pp. 2189-2197, May 2012.

[51] N. Niguchi, K. Hirata, M. Muramatsu and Y. Hayakawa, "Transmission torque characteristics in a magnetic gear," in *Proc. IEEE Int. Elect. Mach. Drives Conf.*, 2010, pp. 1-6.

[52] M. Fukuoka, K. Nakamura and O. Ichinokura, "Experimental tests of surface permanent magnet magnetic gear," in *Proc. Int. Conf. Elec. Mach. And Sys.*, 2012, pp. 1-6.

[53] L. Shah, A. Cruden and B. W. Williams, "A variable speed magnetic gear box using contra-rotating input shafts," *IEEE Trans. Magn.*, vol. 47, no. 2, pp. 431-438, Feb. 2011.

[54] N. W. Frank and H. A. Toliyat, "Analysis of the concentric planetary magnetic gear with strengthened stator and interior permanent magnet inner rotor," *IEEE Trans. Ind. Appl.*, vol. 47, no. 4, pp. 1652-1660, July-Aug. 2011.

[55] L Brönn, R-J. Wang, and M. J. Kamper, "Development of a shutter type magnetic gear," in *Proc. Southern African Universities Power Eng. Conf.*, 2010, pp. 78-82.

[56] L. Jian, K. T. Chau, Y. Gong, J. Z. Jiang, C. Yu and W. Li, "Comparison of coaxial magnetic gears with different topologies," *IEEE Trans. Magn.*, vol. 45, no. 10, pp. 4526-4529, Oct. 2009.

[57] X. Liu, K. T. Chau, J. Z. Jiang, and C. Yu, "Design and analysis of interior-magnet outer-rotor concentric magnetic gears," in *J. Appl. Phys.*, vol. 105, no. 7, pp. 1-3, 2009.

[58] P. O. Rasmussen, T. O. Andersen, F. T. Jørgensen and O. Nielsen, "Development of a high-performance magnetic gear," *IEEE Trans. Ind. Appl.*, vol. 41, no. 3, pp. 764-770, May-June 2005.

[59] K. Atallah, S. D. Calverley and D. Howe, "Design, analysis and realisation of a high-performance magnetic gear," in *Proc. Elec. Power App.*, vol. 151, no. 2, pp. 135-143, Mar. 2004.

[60] P. M. Tlali, S. Gerber and R. Wang, "Optimal design of an outer-stator magnetically geared permanent magnet machine," *IEEE Trans. Magn.*, vol. 52, no. 2, pp. 1-10, Feb. 2016.

[61] W. Zhao, J. Liu, J. Ji, G. Liu and Z. Ling, "Comparison of coaxial magnetic gears with and without magnetic conducting ring," *IEEE Trans. Appl. Supercond.*, vol. 26, no. 4, pp. 1-5, June 2016.

[62] S. Gerber and R. Wang, "Design and evaluation of a magnetically geared PM machine," *IEEE Trans. Magn.*, vol. 51, no. 8, pp. 1-10, Aug. 2015.

[63] S. Gerber and R-J. Wang, "Design of a magnetically geared PM machine," in *Proc. Int. Conf. Power Eng., Energy and Elect. Drives*, 2013, pp. 852-857.

[64] R. Wang, L. Brönn, S. Gerber and P. M. Tlali, "Design and evaluation of a disc-type magnetically geared PM wind generator," in *Proc. Int. Conf. Power Eng. Energy Elec. Drives*, 2013, pp. 1259-1264.

[65] L. Brönn, "Design and Performance Evaluation of a Magnetically Geared Axial-Flux Permanent Magnet Generator," M.Sc. thesis, Dept. Elect. and Electron. Eng., Stellenbosch Univ., Matieland, South Africa, 2012.

[66] K. Atallah, J. Wang, S. D. Calverley and S. Duggan, "Design and operation of a magnetic continuously variable transmission," *IEEE Trans. Ind. Appl.*, vol. 48, no. 4, pp. 1288-1295, July-Aug. 2012.
[67] L. Jian, K. T. Chau and J. Z. Jiang, "A magnetic-geared outer-rotor permanent-magnet brushless machine for wind power generation," *IEEE Trans. Ind. Appl.*, vol. 45, no. 3, pp. 954-962, May-June 2009.
[68] K. Atallah, J. Rens, S. Mezani and D. Howe, "A novel "pseudo" direct-drive brushless permanent magnet machine," *IEEE Trans. Magn.*, vol. 44, no. 11, pp. 4349-4352, Nov. 2008.
[69] S. Du, Y. Zhang, and J. Jiang, "Research on a novel combined permanent magnet electrical machine," in *Proc. Int. Conf. Elec. Mach. and Sys.*, 2008, pp. 3564-3567.
[70] P. M. Tlali, R. Wang and S. Gerber, "Magnetic gear technologies: a review," in *Proc. Int. Conf. Elect. Mach.*, 2014, pp. 544-550.
[71] Z. Q. Zhu, H. Y. Li, R. Deodhar, A. Pride and T. Sasaki, "Recent developments and comparative study of magnetically geared machines," in *CES Trans. Elect. Mach. and Sys.*, vol. 2, no. 1, pp. 13-22, March 2018.
[72] S. Ahmadreza Afsari, H. Heydari and B. Dianati, "Cogging torque mitigation in axial flux magnetic gear system based on skew effects using an improved quasi 3-D analytical method," *IEEE Trans. Magn.*, vol. 51, no. 9, pp. 1-11, Sept. 2015.
[73] H. Zaytoon, A. S. Abdel-Khalik, S. Ahmed and A. Massoud, "Cogging torque reduction of axial magnetic gearbox using pole pairing technique," *IEEE Int. Conf. Ind. Technol.*, 2015, pp. 652-657.
[74] S. J. Kim, E. Park, S. Jung and Y. Kim, "Transfer torque performance comparison in coaxial magnetic gears with different flux-modulator shapes," *IEEE Trans. Magn.*, vol. 53, no. 6, pp. 1-4, June 2017.
[75] Y. Zhan, L. Ma, K. Wang, H. Zhao, G. Xu and N. Ding, "Torque analysis of concentric magnetic gear with interconnected flux modulators," *IEEE Trans. Magn.*, vol. 55, no. 6, pp. 1-4, June 2019.
[76] S. A. Afsari Kashani, "Rotor pole design of radial flux magnetic gear for reduction of flux density harmonics and cogging torque," *IEEE Trans. Appl. Supercond.*, vol. 29, no. 8, pp. 1-8, Dec. 2019.
[77] T. F. Tallerico, Z. A. Cameron and J. J. Scheidler, "Design of a magnetic gear for NASA's Vertical Lift Quadrotor concept vehicle," in *Proc. AIAA/IEEE Elect. Aircraft Technol. Symp.*, 2019, pp. 1-21.
[78] N. W. Frank and H. A. Toliyat, "Gearing ratios of a magnetic gear for wind turbines," in *Proc. IEEE Int. Elect. Mach. Drives Conf.*, 2009, pp. 1224-1230.
[79] T. V. Frandsen and P. O. Rasmussen, "Slip torque investigation and magnetic redesign of motor integrated permanent magnet gear," in *Proc. Int. Conf. Elec. Mach. and Sys.*, 2015, pp. 929-935.
[80] A. Rahideh, A. A. Vahaj, M. Mardaneh and T. Lubin, "Two-dimensional analytical investigation of the parameters and the effects of magnetisation patterns on the performance of coaxial magnetic gears," in *IET Elect. Sys. in Transport.*, vol. 7, no. 3, pp. 230-245, 9 2017.
[81] M. Johnson, M. C. Gardner and H. A. Toliyat, "Design comparison of NdFeB and ferrite radial flux surface permanent magnet coaxial magnetic gears," *IEEE Trans. Ind. Appl.*, vol. 54, no. 2, pp. 1254-1263, Mar.-Apr. 2018.
[82] M. C. Gardner, B. E. Jack, M. Johnson and H. A. Toliyat, "Comparison of surface mounted permanent magnet coaxial radial flux magnetic gears independently optimized for volume, cost, and mass," *IEEE Trans. Ind. Appl.*, vol. 54, no. 3, pp. 2237-2245, May-June 2018.
[83] E. Gouda, S. Mezani, L. Baghli, and A. Rezzoug, "Comparative study between mechanical and magnetic planetary gears," *IEEE Trans. Magn.*, vol. 47, pp. 439-450, 2011.
[84] K. Aiso, K. Akatsu, Y. Aoyama, "A novel reluctance magnetic gear for high-speed motor," *IEEE Trans. Ind. Appl.*, vol. 55, no. 3, pp. 2690- 2699, May/Jun. 2019.
[85] A. Al-Qarni, F. Wu and A. El-Refaie, "High-torque-density low-cost magnetic gear utilizing hybrid magnets and advanced materials," in *Proc. IEEE Int. Elect. Mach. Drives Conf.*, 2019, pp. 225-232.
[86] E. Park, C. Kim, S. Jung and Y. Kim, "Dual magnetic gear for improved power density in high-gear-ratio applications," in *Proc. Int. Conf. Elec. Mach. and Sys.*, 2018, pp. 2529-2532.
[87] Z. Q. Zhu and D. Howe, "Influence of design parameters on cogging torque in permanent magnet machines," *IEEE Trans. Energy Convers.*, vol. 15, no. 4, pp. 407-412, Dec. 2000.
[88] S. A. Afsari, H. Heydari and B. Dianati, "Cogging torque minimization in double sided axial flux magnetic gear," in *Proc. Power Electron. and Drive Sys. and Tech. Conf.*, 2015, pp. 71-76.
[89] M. C. Gardner, M. Johnson and H. A. Toliyat, "Comparison of surface permanent magnet axial and radial flux coaxial magnetic gears," *IEEE Trans. Energy Conv.*, vol. 33, no. 4, pp. 2250-2259, Dec. 2018.
[90] D. J. Evans and Z. Q. Zhu, "Influence of design parameters on magnetic gear's torque capability," in *Proc. IEEE Int. Elect. Mach. Drives Conf.*, 2011, pp. 1403-1408.
[91] M. C. Gardner, M. Johnson and H. A. Toliyat, "Analysis of high gear ratio capabilities for single-stage, series multistage, and compound differential coaxial magnetic gears," *IEEE Trans. Energy Convers.*, vol. 34, no. 2, pp. 665-672, June 2019.
[92] S. Gerber and R-J. Wang, "Analysis of the end-effects in magnetic gears and magnetically geared machines," in *Proc. IEEE Int. Conf. Elect. Mach.*, 2014, pp. 396–402.

Bryton Praslicka (S' 20) earned his B.S. in electrical engineering from Texas A&M University, College Station, Texas in 2019. He is currently pursuing a Ph.D. in electrical engineering while working in the Advanced Electric Machines and Power Electronics Laboratory at Texas A&M University. His research interests include the optimal design and control of electric machines, magnetic gears, and magnetically geared machines.

Matthew C. Gardner (S'15, M'19) earned his B.S. in electrical engineering from Baylor University, Waco, Texas in 2014. He earned his Ph.D. in electrical engineering from Texas A&M University, College Station, Texas in 2019. In August 2020, he joined the University of Texas at Dallas, where he is an assistant professor. His research interests include optimal design and control of electric machines and magnetic gears.

Matthew Johnson (S'13, M'17) earned his B.S. and Ph.D. both in electrical engineering from Texas A&M University, College Station, Texas, in 2011 and 2017, respectively. He is currently an electronics engineer for the U.S. Army Research Laboratory. His research interests include the design and control of electric machines and magnetic gears.

Hamid A. Toliyat (S'13, M'17) (S'87, M'91, SM'96, F'08) received the B.S, degree from Sharif University of Technology, Tehran, Iran in 1982, the M.S. degree from West Virginia University, Morgantown, WV in 1986, and the Ph.D. degree from University of Wisconsin–Madison, Madison, WI in 1991, all in electrical engineering. In March 1994 he joined the Department of Electrical and Computer Engineering, Texas A&M University where he is currently the Raytheon endowed professor of electrical engineering. Dr. Toliyat has many papers and awards to his name, including the Nikola Tesla Field Award.